Contraction pressure analysis using optical imaging in normal and MYBPC3-mutated hiPSC-derived cardiomyocytes grown on matrices with tunable stiffness

Matthijs Snelders [a,1], Iris H. Koedijk [a,1], Julia Schirmer [b], Otto Mulleners [a], Juancito van Leeuwen [a], Nathalie P. de Wagenaar [a,c], Oscar Bartulos [d], Pieter Voskamp [d], Stefan Braam [d], Zeno Guttenberg [b], A.H. Jan Danser [e], Danielle Majoor-Krakauer [f], Erik Meijering [g], Ingrid van der Pluijm [a,h], Jeroen Essers [a,h,i,*]

[a] Department of Molecular Genetics, Erasmus MC, Rotterdam, the Netherlands
[b] ibidi GmbH, Gräfelfing, Germany
[c] Department of Cardiology, Erasmus MC, Rotterdam, the Netherlands
[d] Ncardia, Leiden, the Netherlands
[e] Department of Internal Medicine - Pharmacology, Erasmus MC, Rotterdam, the Netherlands
[f] Department of Clinical Genetics, Erasmus MC, Rotterdam, the Netherlands
[g] School of Computer Science and Engineering, University of New South Wales, Sydney, Australia
[h] Department of Vascular Surgery, Erasmus MC, Rotterdam, the Netherlands
[i] Department of Radiotherapy, Erasmus MC, Rotterdam, the Netherlands

A R T I C L E   I N F O

A B S T R A C T

Current *in vivo* disease models and analysis methods for cardiac drug development have been insufficient in providing accurate and reliable predictions of drug efficacy and safety. Here, we propose a custom optical flow-based analysis method to quantitatively measure recordings of contracting cardiomyocytes on polydimethylsiloxane (PDMS), compatible with medium-throughput systems.

Movement of the PDMS was examined by covalently bound fluorescent beads on the PDMS surface, differences caused by increased substrate stiffness were compared, and cells were stimulated with β-agonist. We further validated the system using cardiomyocytes treated with endothelin-1 and compared their contractions against control and cells incubated with receptor antagonist bosentan. After validation we examined two MYBPC3-mutant patient-derived cell lines.

Recordings showed that higher substrate stiffness resulted in higher contractile pressure, while beating frequency remained similar to control. β-agonist stimulation resulted in both higher beating frequency as well as higher pressure values during contraction and relaxation. Cells treated with endothelin-1 showed an increased beating frequency, but a lower contraction pressure. Cells treated with both endothelin-1 and bosentan remained at control level of beating frequency and pressure. Lastly, both MYBPC3-mutant lines showed a higher beating frequency and lower contraction pressure.

Our validated method is capable of automatically quantifying contraction of hiPSC-derived cardiomyocytes on a PDMS substrate of known shear modulus, returning an absolute value. Our method could have major benefits in a medium-throughput setting.

1. Introduction

Heart failure (HF) is a chronic progressive condition in which the heart fails to pump enough blood to fulfill the metabolic demand of the body [1]. Since the 1990s, HF has become an increasing problem and is currently a leading cause of death. An estimated 37.7 million people have been diagnosed with HF worldwide [2]. While drug development has been improving in other fields of medicine, cardiac drug development has seen slower progress over the years [3]. It can take $2 billion and over 12 years of development for a single compound to be

released [4]. This is partly explained by the fact that predicting toxicity is challenging [4]. Mouse models are often used to evaluate drug effects on cardiac function and toxicity, but their translational value is low [5,6]. Hence, there is a growing need for better cardiac disease models. One promising model is the use of patient-specific induced pluripotent stem cells (hiPSC), a renewing source capable of producing billions of cardiomyocyte-like cells [7–9]. Although proper maturation of hiPSC-derived cardiomyocytes (hiPSC-CM) remains a challenge as of this day, hiPSC-CM are able to spontaneously contract and relax periodically and form a monolayer with intact cell-cell junctions. This allows the investigation of cardiotoxicity and phenotypical differences in both healthy and diseased cells in a model that fully mimics patient characteristics.

Coinciding with the development of disease models, many new tools have been developed to quantify contraction profiles of *in vitro* cardiomyocyte monolayers [10,11]. Impedance-based methods rely on electrodes which measure the electrical resistance of the cell membrane [12]. Another method is the use of fluorescence microscopy to measure the molecular mechanisms of contraction, such as calcium influx and action potential [13]. Current optical-based methods using phase-contrast recordings provide a simple, cost-effective way of analyzing contraction [14]. Many analyses are limited to providing quantitative data of velocity. Additionally, many methods lack automation, making analyses of multiple longitudinal experiments a laborious process.

Here, we describe a custom analysis tool based on Lucas-Kanade optical flow to quantify cardiac contraction in a 2D *in vitro* hiPSC-based model. We use the flexible attributes of polydimethylsiloxane (PDMS) to both provide a physiologically relevant environment for the cells, as well as allowing us to calculate the absolute pressures applied by the cells to the PDMS, by using its shear modulus. With our method we aim to improve cardiac drug discovery by developing a medium-throughput system with maximum biological relevance.

We analyzed the contractility of patient-derived hiPSC-CM with *MYBPC3* mutant gene as experimental model for heart failure. *MYBPC3* is localized on chromosome 11p11.2 and encodes an essential component of the sarcomere. Cardiac MyBP-C (cMyBP-C), the protein encoded by *MYBPC3* gene, functions as a linker between the thick and thin filaments [15]. Mutations in *MYBPC3* are associated with hypertrophic cardiomyopathy and dilated cardiomyopathy (HCM and DCM, respectively). The heterozygous mutation p.Ser311* results in an early stop codon and the production of truncated MYBPC-3 proteins, resulting in haploinsufficiency [16–19]. The p.Trp792ValfsX41 mutation results in familial hypertrophic cardiomyopathy with higher survival rates than other mutations in sarcomeric proteins [20,21]. Both mutations contribute to impaired sarcomere and myocardial contractility and subsequent dilated or hypertrophic compensation of the myocardium reducing functional cardiac output [18,19,22]. We hypothesized that the HCM cells would show aberrant contraction with reduced contractile pressure, and expected our analysis to detect the differences between our two HCM cell lines and their respective healthy control cardiomyocytes *in vitro*.

2. Methods

2.1. PDMS slide preparation

We produced the custom-made PDMS slides using the Angiogenesis μ-slides (#81506, ibidi, Gräfelfing, Germany). A two-component based silicone gel (NuSil MED-6340, Polymer Systems Technology Limited, High Wycombe, United Kingdom) was used to generate PDMS-based substrates of different stiffnesses. The required stiffness was acquired by mixing the silicone base and curing agent at specific ratios according to a calibration curve kindly provided by the company beniag GmbH, Jülich, Germany. The PDMS mixture was then transferred to a syringe with a dispensing needle and used to fill the wells of the angiogenesis slides until a planar surface was obtained. The PDMS was cross-linked for 16 h at 60°C. The slides were sterilized with ethylene oxide (EO) gassing [23].

The shear modulus ranged from 15 kPa resembling healthy heart tissue, to 100 kPa resembling fibrotic heart tissue [24]. Experiments were performed using 15 kPa slides unless noted otherwise.

2.2. Covalently bound fluorescent beads

Our pressure calculation algorithm was validated by directly detecting the movement of the

PDMS using covalently bound FluoSpheres (latex beads) (cat no. F8806, ThermoFisher, München, Germany). PDMS substrates were first salinized by adding 95% ethanol pH 5.0 + 5% APTES (cat no. 440140, Sigma-Aldrich, Taufkirchen, Germany) to the wells and incubating for 3 min at room temperature. Wells were then washed 5 times with 95% ethanol and vacuum aspirated. Slides were left to dry for 30 min at room temperature.

After salinizing the slides, FluoSpheres were activated; the beads were incubated at a ratio of 1:1200 in coupling buffer (31.1 mmol/L 2-(N-morpholino)ethanesulfonic acid pH 6.0 (cat no. 475893, Sigma-Aldrich), 0.1% Sodium Dodecyl Sulfate, 20 mg/mL N-Hydroxysulfosuccinimide sodium salt (cat no. 56485, Sigma-Aldrich), and 20 mg/mL N-(3-Dimethylaminopropyl)-N′-ethylcarbodiimide hydrochloride (cat no. 03450, Sigma-Aldrich) for 15 min at room temperature. Beads were then added to the wells and incubated for 10 min at room temperature. Afterwards wells were washed with distilled H_2O to rid unbound FluoSpheres from the substrate. Slides were then ready for matrix coating and seeding according to the experimental setup.

2.3. Cell culture

Pluricyte Cardiomyocytes (PCM) were kindly provided by Ncardia. The generation of transgene-free hiPSC from skin fibroblasts of Hypertrophic cardiomyopathy patient 1 (HCM1) carrying the mutation $MYBPC3^{p.Trp792ValfsX41}$ was previously reported [25]. Transgene-free hiPSC were generated from skin fibroblast from a second patient carrying mutations $MYBPC3^{Ser311*}$ and $MYBPC3^{Gly148Arg}$ (HCM2) according to protocol approved by the institutional Medical Ethics Committee. hiPSC lines were maintained on Matrigel-coated plates in mTeSR^{tm}1 (Stemcell Technologies, Vancouver, Canada) for at least 2 passages before differentiation. The Pluricyte Cardiomyocyte Differentiation kit (Ncardia, discontinued) was used to generate hiPSC-derived cardiomyocytes according to manufacturer's protocol.

Cardiomyocytes were cultured on plastic 6-wells plates. PCM were thawed and maintained in Pluricyte Cardiomyocyte Medium (Cat no. PCK-1.5, Ncardia, the Netherlands) according to manufacturer's protocol. Cells were maintained in an incubator at 37°C, 5% CO_2, for 3 days before seeding.

Cardiomyocytes were seeded onto coated PDMS slides. First, PDMS slides were exposed to a 180 nm Deep UV lamp for 10 min to make the surface hydrophilic for the coating. The distance between the slides and the lamp was 5 cm. Immediately after, slides were coated with 100 μg/mL fibronectin (cat no. 354008, Corning, Germany), or 1:100 Matrigel (cat no. 354277, Corning) for 1 hour at 37°C. Slides were stored at 4°C for 3 days. After incubation, cells were dislodged using 10x TrypLE Select (#A12177, Gibco, Germany) and seeded onto the PDMS slides at 15.000 cells per well. Medium was refreshed every other day.

2.4. Drug treatment

In our drug experiments, we induced an aberrant phenotype by increasing beating rate with isoproterenol, and by inducing a hypertrophic-like state with endothelin-1 (ET-1) [26]. In our first experimental model, cells were treated with isoproterenol. 10 days after seeding, medium was supplemented with 0.1, 1 or 10 μmol/L isoproterenol hydrochloride (cat no. I6504, Sigma-Aldrich). After 15 min of incubation cells were imaged.

Table 1

Culturing and imaging setup for each experiment.

Experimental model	Model specifications	Cultured on	Substrate stiffness (kPa)	Resolution (pixels)	Frames per second (fps)	Total frames
Isoproterenol		Fibronectin	15, 100	2048×2048	24	239
Substrate stiffness		Matrigel	15	2048×2048	30	299
Disease and rescue	Dilution series	Matrigel	15	1200×1200	24	239
(ET1 + bosentan)	Disease and rescue	Fibronectin	15	1200×1200	24	239
Disease (Healthy vs HCM)	Trp792fs	Matrigel	15	2048×2048	30	199
	Ser311*/Gly148Arg	Matrigel	20	464×346 (3x binning)	30	299

In our second experimental model, cells were treated with endothelin-1. Pluricyte Cardiomyocyte medium was replaced with glucose-free EmbryoMax FHM Mouse Embryo medium (MR056, Sigma-Aldrich). Cells were allowed to equilibrate to the glucose free environment for 2 days.

Medium was supplemented with 0.1 nM, 1 nM or 10 nmol/L ET-1 (cat no. 05-23-3800, Sigma-Aldrich). After 4 h of incubation a subset of cells was supplemented with 10 μmol/L of the mixed endothelin type A and B receptor blocker bosentan (cat no. SML1265, Sigma-Aldrich). Cells were imaged after 24 h of incubation.

2.5. Imaging

Cells on PDMS slides were imaged in a stage top incubation system (ibidi, Germany) at 37°C, and 5% CO_2. Phase-contrast movies were acquired using a 20x objective on a Nikon Ti-Eclipse widefield microscope using an ORCA Flash 4.0 LT camera (0.33·μm/pixel) (Hamamatsu, Japan). The recordings were made during development of the analysis, which introduced differences in experimental setup and recording conditions for each experiment. This in turn allowed for versatility tests between different recording setups. Details of the experimental setup and movie settings for each individual experiment are listed in Table 1.

2.6. Algorithm development and implementation

hiPSC-derived cardiomyocytes were cultured in monolayer on a flexible PDMS substrate (Fig. 1A). hiPSC-derived cardiomyocytes show cyclic contraction and relaxation, pulling on the substrate. This movement is quantified using the Guassian Window MSE plugin in ImageJ. This method is based on the well documented Lucas-Kanade optical flow method [28]. This method assumes that the displacement of pixels between timepoint t and t +1 is small and is constant within a small neighborhood of pixels. In our analysis, we use the default setting of maximum distance of 7 pixels and a sigma of 4. A least-squares error estimator using a Gaussian weight function is calculated. The resulting displacement is presented as a 2-channel image containing the size of the displacement and the direction of displacement. In our current method, the size of displacement (vector length) is used in further analyses steps; the sum pixel intensity per frame was exported to a.csv file, along with additional parameters such as width and height in pixels, and total area showing displacement in each frame.

The pressure calculations are performed in MATLAB (version R2019b); pixel size, frames per second and substrate shear modulus of PDMS are provided by the user. Selection of the movies is automated and requires the path to the folder containing the .csv files exported by ImageJ, thus processing multiple recordings at once. Pressure calculation is based on the shear modulus of the PDMS substrate as per the following [27]:

$$F = \frac{G \times A \times \Delta x}{l}$$

where F is the force in N, G is the shear modulus in Pa, A is the area of a pixel (m^2), Δx is the total displacement in frame t with respect to frame t-1, and l is the length (depth) of the substrate. F is then divided by the area of moving pixels (m^2) to obtain the average pressure per pixel per frame in N/m^2 (Pa). Due to variation in contractile uniformity, we

normalize the amount of movement to the amount of pixels moving per frame.

Because optical flow outputs a velocity, we depict the pressure difference as ΔPa plotted against time (Fig. 1B). Extremes are automatically identified as peaks by taking the derivative of the graph and finding the values on the x-axis where the derivative changes from positive to negative, and by an automatically calculated threshold to distinguish peak displacement from background noise. Peaks are identified as either a contraction or relaxation based on the time between 3 following peaks; shorter times between peaks 1 and 2 compared to peaks 2 and 3 will identify peak 1 and 3 as contraction and peak 2 as relaxation. The threshold and peak order can be adjusted manually by the user to intervene when the analysis fails to properly classify contraction or relaxation peaks. After confirming proper peak detection, the time and pressure parameters are calculated; time parameters show the mean time to fully contract and relax, the mean time before contracting or relaxing, and the overall consistency of contraction intervals in seconds. Pressure parameters include mean and maximum contraction and relaxation pressures in Pa, and the maximum speed of contraction and relaxation in dP/dt.

2.7. Code availability

Vector fields were generated from the movies using the implemented Fiji plugin Windows Gaussian MSE (Fiji version 1.53c). Downstream processing of the output was written in a Fiji macro. Raw data was analyzed in MATLAB through our custom automated analysis. Source code is available in the online data repository.

2.8. Statistics

Statistical differences were tested using a two-tailed t-test, one-way ANOVA or two-way ANOVA for unpaired measurements (indicated for each experiment in the legend). The *p*-values obtained from two-tailed pairwise comparisons were corrected for multiple testing using the Bonferroni method. Statistical analyses were performed with Graphpad Prism (v9.0.1). *p*-values less than 0.05 were considered statistically significant and are indicated with an asterisk (*). N values represent technical replicates.

3. Results

3.1. Analysis validation

The ability of the hiPSC-derived cardiomyocytes to apply pressure to the PDMS substrate and the ability of the analysis to detect and analyze these contractions was initially assessed using three experimental conditions: [1] movement of the PDMS using fluorescent beads covalently bound to the PDMS surface, [2] fibrosis of the heart simulated by using variable substrate stiffnesses, and [3] induced tachycardia by addition of isoproterenol. We have shown example peak patterns in supplemental Fig. 1 which are used to calculate the different parameters.

First, we evaluated how much movement in a phase-contrast recording contributed to actual motion of the PDMS. Wells containing a PDMS substrate coated with covalently bound fluorescent beads (TxRed) were seeded with PCM and recordings were made using phase-contrast. The
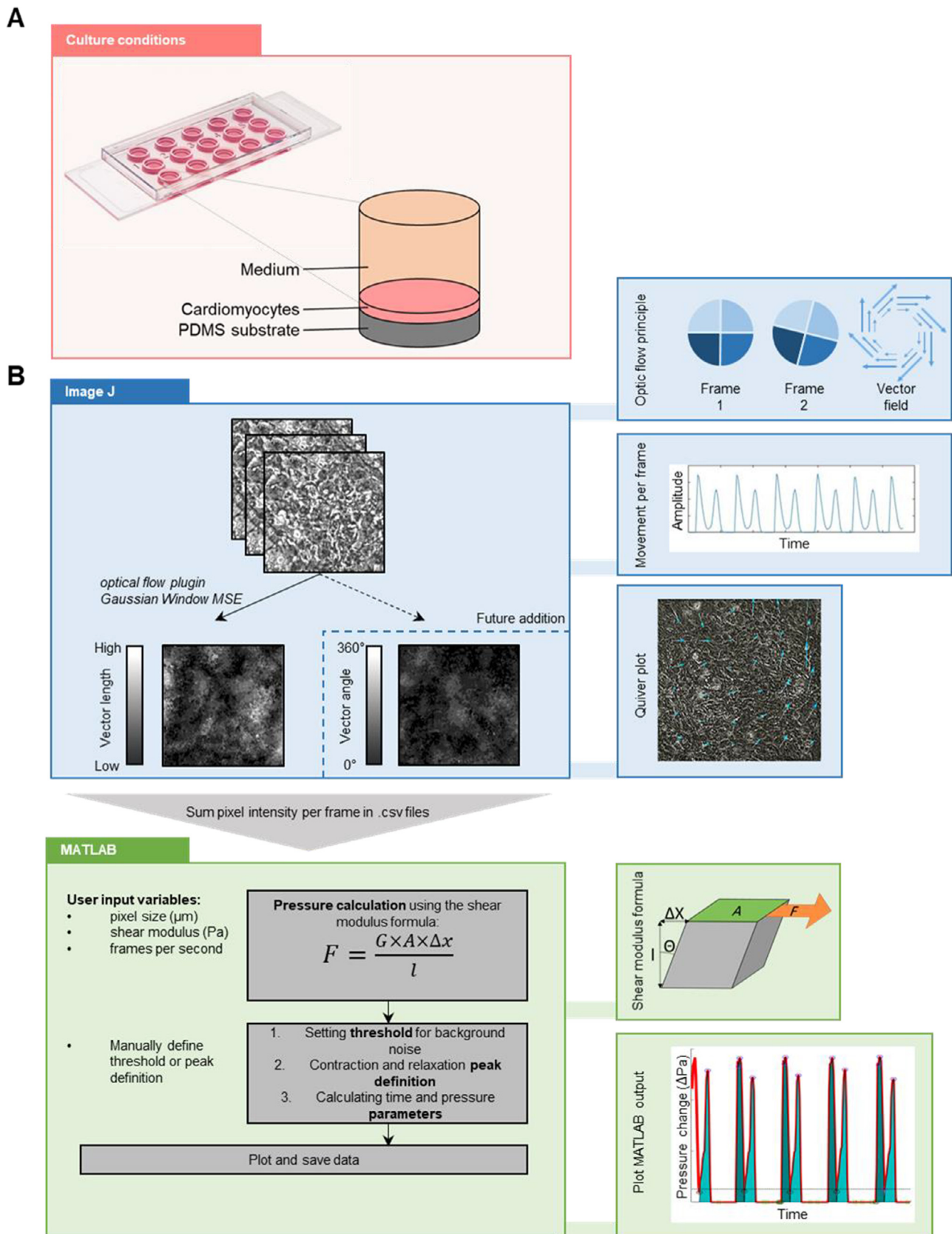
Fig. 1. Contraction analysis workflow. (A) Experimental culturing setup. Cardiomyocytes are grown on a flexible PDMS substrate in a μ-angiogenesis slide well (ibidi). Confluent sections of each well were used for phase-contrast imaging. **(B)** Schematic overview of the contraction analysis workflow. Cardiomyocyte movies are imported in ImageJ and the Gaussian Window MSE optical flow plugin is used to analyze pixel displacement. Length and direction of pixel displacement are stored in two separate files as a vector field. The sum of pixel intensity (movement per frame) is exported to a.csv file, along with additional information such as movie width and height in pixels, and total area showing displacement in each frame. Force calculations are performed and converted to pressure in MATLAB using the shear modulus formula where G is the shear modulus (Pa), A is the area of a pixel (m^2), x is the total displacement in frame t over frame t-1, and l is the length/depth of the substrate. The resulting pressure change F (ΔPa) is then plotted.
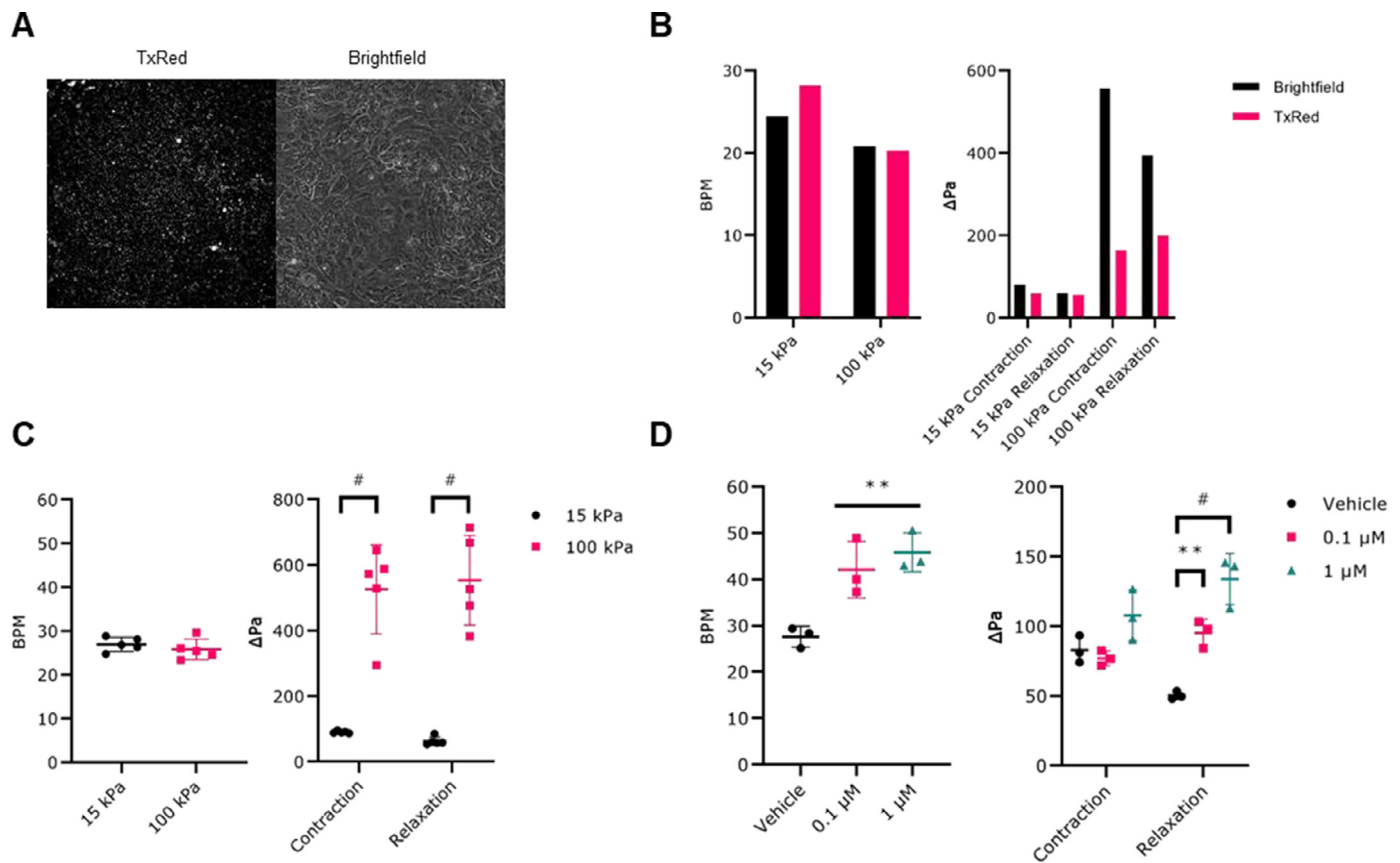
Fig. 2. Validation of optical flow analysis by application to multiple experiments. (A) TxRed image showing the orientation of fluorescent beads in PDMS substrate and a corresponding phase-contrast image depicting cardiomyocyte orientation on top of PDMS substrate (B) Comparison of beating rate and pressure applied to the substrate (stiffness of 15 kPa and 100 kPa) by contracting cardiomyocytes by analyzing movement of a TxRed (fluorescent beads) movie and the phase-contrast (cardiomyocytes) movie. Data consist of 1 technical replicate in each condition. (C) Effects of substrate stiffness on beating rate and pressure applied to the substrate. Data consist of 5 technical replicates in each condition. Data represent mean with SD. Significance shown in comparison with 15 kPa control. Two-tailed t-test (beating rate) and two-way ANOVA with Bonferroni correction (pressure). #; $p \leq 0.001$. (D) Effects of isoproterenol on beating rate and pressure applied to the substrate by contracting cardiomyocytes. Data consist of 3 technical replicates in each condition. Data represent mean with SD. Significance is shown in comparison with 0 μM control. One-way (beating rate) and two-way (pressure) ANOVA with Bonferroni correction. *; $p \leq 0.05$, **; $p \leq 0.01$, #; $p \leq 0.001$.

recordings were made on 15 kPa stiffness resembling healthy human heart conditions, and 100 kPa stiffness resembling fibrotic human heart conditions. Contraction pressures were compared between both phase-contrast and fluorescence recordings (Fig. 2A). No differences in beating rate were recorded between phase-contrast and fluorescence movies, for both 15 kPa and 100 kPa stiffness (Fig. 2B). Overall, the fluorescent recordings showed a lower amount of pressure when compared to phase-contrast recordings on 15 kPa stiffness (Fig. 2B, 60 Pa vs. 70 Pa) and 100 kPa (Fig. 2B, 180 Pa vs. 480 Pa).

Next, we determined the effect of substrate stiffness on contraction in recordings of 15 and 100 kPa stiffness. No difference in beating rate could be detected in both 15 and 100 kPa conditions. Contraction and relaxation pressures was on average significantly higher in the 100 kPa condition compared to 15 kPa (Fig. 2C, 570 vs. 75 Pa; $p \leq 0.001$).

To validate our method against varying beating rates, we assessed the effects of the β-agonist isoproterenol. PCM cells were subjected to vehicle, 0.1 μM or 1 μM isoproterenol for 24 h. A concentration of 0.1 μM isoproterenol showed a higher beating frequency compared to the vehicle control (42.1 BPM vs. 27.6 BPM; $p \leq 0.01$). The 1 μM dose further increased this (45.8 BPM vs. 27.6 BPM; $p \leq 0.005$), which could be indicative of a dose-dependent effect (Fig. 2D, $p \leq 0.01$). We looked into the temporal parameters regarding contraction and relaxation (Fig. 4A). We found that the increase in beating rate could be a result of both shorter contraction and relaxation times. Both times were ~0.4 s in ve-

hicle and ~0.2 s in treated samples, but this difference was not significant.

During contraction, a higher pressure was seen in the 1 μM condition compared to the vehicle (108 Pa vs. 83 Pa; $p = 0.06$), but not for the 0.1 μM treated cells (77 Pa vs. 83 Pa; $p > 0.99$). During relaxation, pressure changes were higher for both 0.1 μM (95.2 Pa/s vs 50.4 Pa; $p \leq 0.001$) and 1 μM (133.9 Pa vs 50.4 Pa; $p \leq 0.001$) compared to vehicle.

3.2. Application in disease phenotypes in vitro

Having shown that our analysis can detect hiPSC-derived cardiomyocyte contractions in line with expectations of three independent experimental conditions, we next sought to demonstrate its ability in more complex disease mechanics. Movies of two different disease mechanics were analyzed; [1] hypertrophy induced by endothelin-1 and [2] hypertrophic cardiomyopathy caused by mutations in *MYBPC3*.

In the first model, healthy PCM cells were incubated with ET-1 to induce a hypertrophic-like state. Cells were grown on 15 kPa PDMS and were incubated with concentrations of vehicle, 5 nM, 10 nM or 100 nM ET-1 in glucose-free medium for 24 h. ET-1 showed a positive chronotropic effect (increased beating rate), increasing beating rates from 16.5 BPM in the vehicle control to 24.9 BPM at concentrations of 5 nM and higher (Fig. 3A, $p \leq 0.001$), while showing a negative inotropic effect (lowering contraction and relaxation pressures) compared
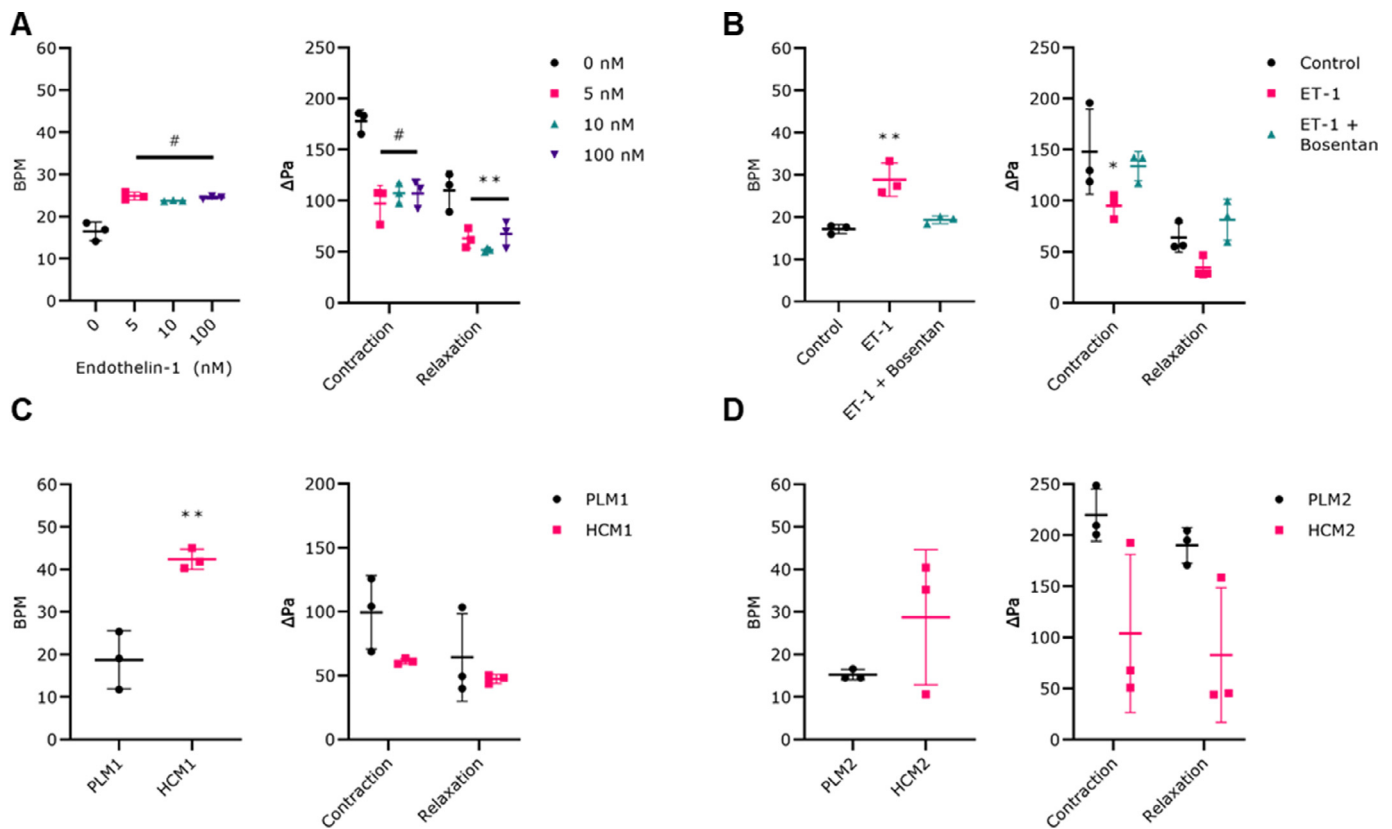
Fig. 3. Application to *in vitro* and *in vivo* disease phenotypes. Data represent mean with SD in all graphs. (A) Effects of ET1 on beating rate and pressure applied to the substrate by contracting cardiomyocytes. Data consist of 3 technical replicates in each condition. Significance shown in comparison with MR056 control. One-way (left) and two-way (right) ANOVA with Bonferroni correction. **; $p \leq 0.01$, #; $p \leq 0.001$. (B) Effects of ET1 and subsequent treatment with Bosentan on beating rate (left) and pressure applied to the substrate (right) by contracting cardiomyocytes. Data consist of 3 technical replicates in each condition. Significance shown in comparison with MR056 control. One-way (left) and two-way (right) ANOVA with Bonferroni correction. *; $p \leq 0.05$, **; $p \leq 0.01$. (C and D) Comparison between healthy and hypertrophic cardiomyopathy cardiomyocytes of beating rate and pressure applied to the substrate. PLM1 = control cardiomyocyte line 1, HCM1 = hypertrophic cardiomyopathy line 1 carrying a Trp792fs mutation in MYBPC3, PLM2 = control cardiomyocyte line 2, HCM2 = hypertrophic cardiomyopathy line 2 carrying a Ser311*/Gly148Arg mutation in MYBPC3. Data consist of 3 technical replicates in each condition. Significance shown in comparison with healthy control. Two-tailed *t*-test (left) and two-way (right) ANOVA with Bonferroni correction. **; $p \leq 0.01$.
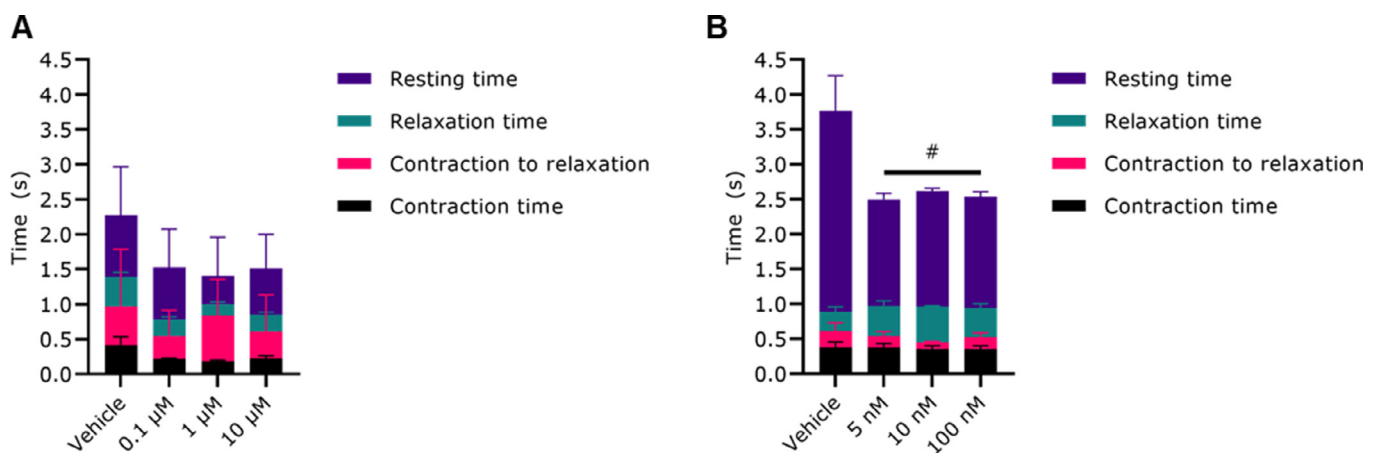

Fig. 4. Temporal parameters for isoproterenol (A) and endothelin-1 (B) recordings at different concentrations. Data represent mean with SD of three technical replicates. Two-way ANOVA with Bonferroni correction. #; $p \leq 0.001$.

to vehicle (Fig. 3A, $p \leq 0.001$ and $p = 0.003$). For this experiment, we also examined the temporal parameters regarding contraction and relaxation, and found that the resting period between contractions was significantly reduced from ~3.7 s to ~2.5 s in the ET-1 treated samples (Fig. 4b, $p \leq 0.001$).

To further evaluate the output parameters of our *in vitro* cardiomyocyte system, a disease-treatment scenario was analyzed. As before,

PCM cells were incubated with 10 nM ET-1 for 24 h. Cells were then split into two groups: one group received the same treatment with ET-1, the other received ET-1 with addition of 10 nM bosentan. After 24 h of incubation, bosentan was added to prevent the ET-1 induced chronotropic and inotropic effects. As before, ET-1 showed a positive chronotropic effect (Fig. 3B, $p = 0.002$) while ET-1 + bosentan treated cells showed no difference compared to control ($p = 0.60$). Contraction and relaxation

pressures were also not different compared to control after treatment with bosentan (ET-1; $p = 0.02$, ET-1 + bosentan; $p = 0.87$).

As an experiment with unknown outcome, two hypertrophic cardiomyopathy patient cell lines were examined in separate experiments. These cell lines carry a mutant *MYBPC3* allele causing haploinsufficiency; *MYBPC3*^{Trp792fs} (HCM1) and *MYBPC3*^{Ser311*} / *MYBPC3*^{Gly148Arg} (HCM2). HCM1 and control hiPSC-CM were seeded on PDMS 15 kPa, and HCM2 and control hiPSC-CM were seeded on 20 kPa PDMS due to differences in experimental setup. Albeit different in stiffness, both 15 kPa and 20 kPa are representative of healthy physiological stiffness of the adult human heart and were therefore considered valid controls in their respective experiment. Both HCM1 and HCM2 cells showed a higher beating rate compared to their respective healthy control (Fig. 3C, HCM1 42 BPM vs. 18 BPM; $p \leq 0.005$, HCM2 29 BPM vs. 15 BPM; $p = 0.22$). Additionally, contraction and relaxation pressures on average showed signs of being lowered in both patient cell lines compared to their respective healthy control, although this effect was not significant (Fig. 3C and D, HCM1 54 Pa vs. 82 Pa; $p = 0.14$, HCM2 93 Pa vs. 205 Pa; $p = 0.06$).

4. Discussion

Cardiac drug development has suffered from high costs with low rates of success during clinical trials, greatly hampering progress of medical care for cardiac diseases. One of the major contributors to this situation is the use of pre-clinical animal models with low translational value [3–5]. To produce output parameters in a pre-clinical *in vitro* setting which are comparable to *in vivo* conditions, it is essential to devise a versatile and accurate method for quantification of cardiac contractility. Here, we developed and validated a custom optical flow-based analysis method to quantitatively determine the absolute contractile pressures applied by hiPSC-derived cardiomyocytes, using the flexible properties of PDMS and its respective shear modulus. More importantly, our method is nearly fully automated and requires minimal intervention. Due to how the data is stored in a text file rather than as images, our analysis is efficient in rapidly storing and analyzing data, which would make its potential more apparent in a medium-throughput setting.

The principle of our method relies on the flexible properties of polydimethylsiloxane (PDMS). Cardiomyocytes seeded on this flexible substrate pull on the substrate during contraction. As the shear modulus of the PDMS can be estimated based on the mixing ratio of the reagent and polymer, we can then directly translate movement recorded using phase-contrast to absolute pressures in Pascal. Movement is extracted through the Lucas-Kanade optical flow method and is stored in table format with negligible loss of information. This assures that downstream analyses can be performed within seconds, providing data on contraction- and relaxation pressures and timing, with minimal storage capacity requirements.

We validated our method by comparing the motion in phase-contrast recordings of contracting cardiomyocytes, with the motion of fluorescence recordings of covalently bound beads on the PDMS surface of the same sample [29]. We predominantly used 15 kPa in our experiments as this coincides with the native human healthy heart tissue stiffness range of 15–23 kPa. A 15 kPa model has been previously shown to accurately resemble the native environmental extracellular matrix stiffness *in vivo* [30,31]. Durán-Pastén et al. previously showed that cardiomyocytes adhere to a soft substrate resembling the native environment better than to a stiff substrate [32]. Additionally, cells could more properly form a monolayer, resulting in uniform calcium signaling [32].

On our 15 kPa model, bead movement could be detected showing that cardiomyocyte contractions pull on the PDMS substrate. We could not determine a difference in pressure between phase-contrast and fluorescence in this case, and concluded that cardiomyocyte movement directly translates to PDMS movement at 15 kPa stiffness, and therefore allows absolute quantification of pressure.

We performed the same experiment using a 100 kPa PDMS substrate, representing fibrotic heart tissue [27,30,33]. In contrast to 15 kPa, we found a nearly threefold decrease in motion of the fluorescent beads recording compared to the phase-contrast recording at 100 kPa stiffness. We assumed that this is caused by movement of both cells and surface in the phase-contrast recordings. On a stiffer substrate, the cardiomyocytes must apply more pressure to get the same amount of movement. To calculate the absolute pressure, we assumed that the movement in the recordings is representative of the movement of the surface itself, but this seems not the case at higher stiffnesses. Thus, when using higher stiffnesses our current method overestimates the pressure applied to the surface. As of this moment we have been unable to further investigate this (non-)linear relationship between stiffness and cell movement. As opposed to the single-cell analysis reported by Czirok et al. [14], we perform analysis of the entire field of view. This introduces movement caused by cells pulling on one another as well as on the substrate. Both stiffness and cell-cell contact could explain this overestimation. Further studies are required to correct for stiffness and cell-cell contact, so that this can be incorporated into the pressure calculations.

We further validated the system by inducing parametric changes which were expected to be distinguishable to control conditions after analysis. First, we subjected cardiomyocytes to the β-agonist isoproterenol. Treatment of cardiomyocytes with isoproterenol resulted in detectable increases in beating rate and increased pressure values compared to control, a finding which is consistent with previous studies [34–36]. Beating rates increased by roughly 30% at concentrations as low as 0.1 μM isoproterenol, and increased in a dose-dependent manner. We recorded the contractions at 24 frames per second, which resulted in acceptable accuracy and detection of both contraction and relaxation phases at beating rates of 60 beats per minute. We did notice that relaxation pressure changed more strongly in cells treated with isoproterenol than in control, exceeding that of their respective contraction pressure change. At this point we were unsure whether this could be contributed by the low recording speed, or because cells relax more rapidly after isoproterenol treatment (Fig. 4A, not significant).

We then subjected cardiomyocytes to ET-1. ET-1 has known vasoconstrictor actions and has previously been successfully used to mimic the hypertrophic phenotype in human adult and hiPSC- CMs [37–41]. In addition, it was shown that ET-1 increased the presence of myofibrillar disarray in hiPSC-derived CMs, resulting in decreased contraction amplitude in mouse embryonic stem cell-derived cardiomyocytes and an increase in beating frequency in hiPSC-CM [37,42,43]. Our analysis was able to detect an increase in beating rate and a decrease in both contraction and relaxation pressure after treatment with ET-1, consistent with the known mechanism of action of the compound. We subsequently rescued the diseased state with the ET-1 receptor antagonist bosentan. The addition of bosentan attenuated these effects and produced results comparable to controls. We conclude that our analysis is able to distinguish between healthy and diseased conditions in this experimental setup.

Considering the ultimate endpoint of this contraction analysis as a means to discover new cardiac drugs in a medium-throughput setting, our analysis was also validated using hiPSC-derived cardiomyocytes of patients diagnosed with hypertrophic cardiomyopathy, carrying mutations in *MYBPC3*. The mutations we studied, p.Trp792ValfsX41 and p.Ser311*, lead to C-terminally truncated proteins and were predicted to cause haploinsufficiency [16,17,44]. Physiological studies have shown that truncating mutations are associated with cardiomyocyte hypertrophy, reduced pressure-generating capacity of cardiomyocytes and reduced myofibril density [17]. On a general note, contraction analysis of both HCM models in this study revealed a trend of higher beating frequency and lower contraction and relaxation pressures than in healthy controls. However, in the p.Trp792ValfsX41 HCM model only beating frequency showed an increase, while a reduction in contraction pressure was only indicative compared to the healthy control cardiomyocytes. These pressure measurements are supported by previous results of de-

creased contractile pressures in patient hiPSC-derived cardiomyocytes carrying truncated mutations at the single-cell level [45,46].

Overall, our contraction analysis provided the expected correlations between known inputs and outputs in our presented experimental models. Several challenges still need to be considered in the process of developing a user-friendly, accurate, and fully automated analysis for quantification of contractile function in cardiac disease phenotypes. The current method requires two programs, ImageJ and MATLAB, to generate output parameters. An easy-to-use contraction analysis for medium-throughput drug screening would in the future ideally require only one analysis program.

Optical flow is a basic method of calculating movement of a given pixel on a frame-to-frame basis, which is employed on several assumptions. One assumption is that the signal intensity remains constant from frame to frame. In transmission and phase-contrast microscopy, contraction of cells by itself causes shifts in signal intensity by compressing the membrane, making the edges of the cells appear darker and possibly affecting the level of pixel displacement. Also, shadows might be picked up as pixel displacement. Image registration was evaluated as an alternative measuring method [47]. The method uses histogram-based tracking of subsections of a movie, using a reference frame to better estimate the movement. At this time, we found no significant difference in calculation accuracy between optical flow and the image registration method (unpublished data), placing optical flow favorable for its faster processing.

In light of previously published optical flow-based analyses, our method, in its current form, provides a rapid, automated workflow for drug screening with the intent to determine differences in contractile phenotype. Several analysis software analysis tools have been developed over the past decades. One example, developed by Toepfer et al., analyzes the contraction of sarcomeres within the cell [48]. The method requires fluorescently tagged sarcomeres and studies sarcomere contraction specifically. Sarcomeres, while being the main contractile structure within the cardiomyocytes, do not show the systemic contraction we observe when looking at the complete cell or heart. Other mechanisms such as the composition of the skeletal structure within the cell play a role in contraction as well. Unless interested in the sarcomere specifically, looking at the whole cell provides more relevant information when analyzing contraction movement. Other optical flow-based methods from Kumar et al. and Scalzo et al. provide the contractions as either an arbitrary unit or as a velocity [49,50].

Our method uses movement information to determine the overall contraction pattern within a recording. In its current state, we do not use the directionality of movement, nor do we provide spatial information on the areas of beating cardiomyocytes, as seen in the works of Czirok et al [14]. In the future, we aim to examine whether cell alignment and contraction propagation can be added as relevant parameters using the spatial information we currently lack. Additionally, contractile heterogeneity across the field of view was observed. We calculated the coefficient of variation to be approximately 75.84% during peak contraction in our isoproterenol recordings. The origin for this variability could come from various sources; we use iPSC derived cardiomyocytes which, although from a human source, do not represent mature cardiomyocytes. The cells do not form the typical elongated shape. From an experimental standpoint, gaps between cells might be visible, lack of pacing, or insufficient differentiation/selection introduced non-contractile cells. We intend to introduce pacing for future experiments.

We further intend to improve our more detailed time parameters. As of yet, the analysis provides temporal information regarding contraction time, contracted period, relaxation time and resting period (Fig. 4). These parameters, although important, have shown to be variable depending on the experiment. We intend to further optimize this by using a high-speed camera at more than 100 frames per second, so that these hundreds of nanoseconds differences between contractions can be properly quantified.

Absolute pressure can be calculated at a certain time point by adding the pressure derivatives over time. We have been able to achieve this for several recordings (supplemental Fig. 1), but in most cases did not succeed due to the low recording speeds. Once available, we expect to be able to properly quantify absolute pressures at a given time using these outcome parameters.

Regarding computation times, analyzing a recording of 1024×1024×300 could take approximately 5 min to extract the velocities (this is only required one time). After this, the MATLAB code can quantify the results within 3 s, assuming the thresholds were set correctly and peaks were correctly allocated on a previous run, otherwise it would take approximately 1.5 s due to drawing the graph. These runs were performed on a 3.0 GHz 6-core CPU. We are looking into ways to further improve computation times by recoding into a single platform using Python. Different plugins for drawing the graphs would help speed up the processing considerably, as well as comparing different optical-flow based techniques.

In conclusion, our current contraction analysis offers a non-invasive, user-friendly, optical flow-based solution for absolute contractile quantification. Future extensions include applying our method to three-dimensional models consisting of paced and fully mature cardiomyocytes that more accurately resemble the complex integrated diseased phenotype. We believe our method will facilitate research in drug development, personalized medicine and clinical applications.

Sources of funding

Disclosures

None.

Data availability

The raw/processed data required to reproduce these findings cannot be shared at this time due to technical or time limitations.

Declaration of Competing Interest

The authors declare that they have no known competing financial interests or personal relationships that could have appeared to influence the work reported in this paper.

Data availability

Data will be made available on request.

Acknowledgment

Supplementary materials

Supplementary material associated with this article can be found, in the online version, at doi:10.1016/j.bbiosy.2022.100068.

References

[1] Ziaeian B, Fonarow GC. Epidemiology and aetiology of heart failure. Nat. Rev. Cardiol. 2016;13(6):368–78.

[2] Vos T, Flaxman AD, Naghavi M, Lozano R, Michaud C, Ezzati M, et al. Years lived with disability (YLDs) for 1160 sequelae of 289 diseases and injuries 1990-2010: a systematic analysis for the global burden of disease study 2010. Lancet North Am. Ed. 2012;380(9859):2163–96.

[3] Fordyce CB, Roe MT, Ahmad T, Libby P, Borer JS, Hiatt WR, et al. Cardiovascular drug development: is it dead or just hibernating? J. Am. Coll. Cardiol. 2015;65(15):1567–82.

[4] Savoji H, Mohammadi MH, Rafatian N, Toroghi MK, Wang EY, Zhao Y, et al. Cardiovascular disease models: a game changing paradigm in drug discovery and screening. Biomaterials 2019;198:3–26.

[5] Breckenridge R. Heart failure and mouse models. Dis. Model Mech. 2010;3(3-4):138–43.

[6] Yutzey KE, Robbins J. Principles of genetic murine models for cardiac disease. Circulation 2007;115(6):792–9.

[7] Laverty H, Benson C, Cartwright E, Cross M, Garland C, Hammond T, et al. How can we improve our understanding of cardiovascular safety liabilities to develop safer medicines? Br. J. Pharmacol. 2011;163(4):675–93.

[8] Passier R, Orlova V, Mummery C. Complex tissue and disease modeling using hiPSCs. Cell Stem Cell 2016;18(3):309–21.

[9] Bellin M, Marchetto MC, Gage FH, Mummery CL. Induced pluripotent stem cells: the new patient? Nat. Rev. Mol. Cell Biol. 2012;13(11):713–26.

[10] Sala L, van Meer BJ, Tertoolen LGJ, Bakkers J, Bellin M, Davis RP, et al. MUSCLEMOTION: a versatile open software tool to quantify cardiomyocyte and cardiac muscle contraction *in vitro* and *in vivo*. Circ. Res. 2018;122(3):e5–e16.

[11] Reno A, Hunter AW, Li Y, Ye T, Foley AC. Quantification of cardiomyocyte beating frequency using fourier transform analysis. Photonics 2018;5(4):39.

[12] Scott CW, Zhang X, Abi-Gerges N, Lamore SD, Abassi YA, Peters MF. An impedance-based cellular assay using human iPSC-derived cardiomyocytes to quantify modulators of cardiac contractility. Toxicol. Sci. 2014;142(2):331–8.

[13] van Meer BJ, Krotenberg A, Sala L, Davis RP, Eschenhagen T, Denning C, et al. Simultaneous measurement of excitation-contraction coupling parameters identifies mechanisms underlying contractile responses of hiPSC-derived cardiomyocytes. Nat. Commun. 2019;10(1):4325.

[14] Czirok A, Isai DG, Kosa E, Rajasingh S, Kinsey W, Neufeld Z, et al. Optical-flow based non-invasive analysis of cardiomyocyte contractility. Sci. Rep. 2017;7(1):10404.

[15] Mohamed IA, Krishnamoorthy NT, Nasrallah GK, Da'as SI. The role of cardiac myosin binding protein C3 in hypertrophic cardiomyopathy-progress and novel therapeutic opportunities. J. Cell. Physiol. 2017;232(7):1650–9.

[16] Marston S, Copeland O, Jacques A, Livesey K, Tsang V, McKenna WJ, et al. Evidence from human myectomy samples that MYBPC3 mutations cause hypertrophic cardiomyopathy through haploinsufficiency. Circ. Res. 2009;105(3):219–22.

[17] van Dijk SJ, Dooijes D, dos Remedios C, Michels M, Lamers JM, Winegrad S, et al. Cardiac myosin-binding protein c mutations and hypertrophic cardiomyopathy: haploinsufficiency, deranged phosphorylation, and cardiomyocyte dysfunction. Circulation 2009;119(11):1473–83.

[18] Carrier L, Mearini G, Stathopoulou K, Cuello F. Cardiac myosin-binding protein c (MYBPC3) in cardiac pathophysiology. Gene 2015;573(2):188–97.

[19] Flashman E, Redwood C, Moolman-Smook J, Watkins H. Cardiac myosin binding protein C: its role in physiology and disease. Circ. Res. 2004;94(10):1279–89.

[20] Niimura H, Bachinski LL, Sangwatanaroj S, Watkins H, Chudley AE, McKenna W, et al. Mutations in the gene for cardiac myosin-binding protein c and late-onset familial hypertrophic cardiomyopathy. N. Engl. J. Med. 1998;338(18):1248–57.

[21] Moolman JA, Reith S, Uhl K, Bailey S, Gautel M, Jeschke B, et al. A newly created splice donor site in exon 25 of the mybp-c gene is responsible for inherited hypertrophic cardiomyopathy with incomplete disease penetrance. Circulation 2000;101(12):1396–402.

[22] Kaier TE, Alaour B, Marber M. Cardiac myosin-binding protein C-From bench to improved diagnosis of acute myocardial infarction. Cardiovasc. Drugs Ther. 2019;33(2):221–30.

[23] Jin C, Ma C, Yang Z, Lin H. A force measurement method based on flexible pdms grating. Appl. Sci. 2020;10(7):2296.

[24] Herum KM, Lunde IG, McCulloch AD, Christensen G. The Soft- and Hard-Heartedness of cardiac fibroblasts: mechanotransduction signaling pathways in fibrosis of the heart. J Clin Med 2017;6(5).

[25] Dambrot C, Braam SR, Tertoolen LG, Birket M, Atsma DE, Mummery CL. Serum supplemented culture medium masks hypertrophic phenotypes in human pluripotent stem cell derived cardiomyocytes. J. Cell. Mol. Med. 2014;18(8):1509–18.

[26] de Jonge HW, Dekkers DH, Houtsmuller AB, Sharma HS, Lamers JM. Differential signaling and hypertrophic responses in cyclically stretched vs endothelin-1 stimulated neonatal rat cardiomyocytes. Cell Biochem. Biophys. 2007;47(1):21–32.

[27] Mills I, Cvitaš T, Homann K, Kallay N, Kuchitsu K, editors. Physical Chemistry Division: Quantities, Units and Symbols in Physical Chemistry. 2nd ed., 98(4) Oxford: Blackwell Scientific Publications Ltd.; 1994. p. 645.

[28] Fortun D, Bouthemy P, Kervrann C. Optical flow modeling and computation: a survey. Comput. Vision Image Underst. 2015;134:1–21.

[29] Yoshie H, Koushki N, Kaviani R, Tabatabaei M, Rajendran K, Dang Q, Husain A, Yao S, et al. Traction force screening enabled by compliant pdms elastomers. Biophys. J. 2018;114(9):2194 2199.

[30] Rodriguez AG, Han SJ, Regnier M, Sniadecki NJ. Substrate stiffness increases twitch power of neonatal cardiomyocytes in correlation with changes in myofibril structure and intracellular calcium. Biophys. J. 2011;101(10):2455–64.

[31] Engler AJ, Carag-Krieger C, Johnson CP, Raab M, Tang HY, Speicher DW, et al. Embryonic cardiomyocytes beat best on a matrix with heart-like elasticity: scar-like rigidity inhibits beating. J. Cell Sci. 2008;121:3794–802 Pt 22.

[32] Duran-Pasten ML, Cortes D, Valencia-Amaya AE, King S, Gonzalez-Gomez GH, Hautefeuille M. Cell culture platforms with controllable stiffness for chick embryonic cardiomyocytes. Biomimetics 2019;4(2) (Basel).

[33] Ribeiro MC, Slaats RH, Schwach V, Rivera-Arbelaez JM, Tertoolen LGJ, van Meer BJ, et al. A cardiomyocyte show of force: a fluorescent alpha-actinin reporter line sheds light on human cardiomyocyte contractility versus substrate stiffness. J. Mol. Cell Cardiol. 2020;141:54–64.

[34] Mehta A, Chung YY, Ng A, Iskandar F, Atan S, Wei H, et al. Pharmacological response of human cardiomyocytes derived from virus-free induced pluripotent stem cells. Cardiovasc. Res. 2011;91(4):577–86.

[35] Zhao Q, Wang X, Wang S, Song Z, Wang J, Ma J. Cardiotoxicity evaluation using human embryonic stem cells and induced pluripotent stem cell-derived cardiomyocytes. Stem Cell Res. Ther. 2017;8(1):54.

[36] Guo L, Abrams RM, Babiarz JE, Cohen JD, Kameoka S, Sanders MJ, et al. Estimating the risk of drug-induced proarrhythmia using human induced pluripotent stem cell-derived cardiomyocytes. Toxicol. Sci. 2011;123(1):281–9.

[37] Tanaka A, Yuasa S, Mearini G, Egashira T, Seki T, Kodaira M, et al. Endothelin-1 induces myofibrillar disarray and contractile vector variability in hypertrophic cardiomyopathy-induced pluripotent stem cell-derived cardiomyocytes. J. Am. Heart Assoc. 2014;3(6):e001263.

[38] Kockskamper J, von Lewinski D, Khafaga M, Elgner A, Grimm M, Eschenhagen T, et al. The slow force response to stretch in atrial and ventricular myocardium from human heart: functional relevance and subcellular mechanisms. Prog. Biophys. Mol. Biol. 2008;97(2-3):250–67.

[39] Yanagisawa M, Kurihara H, Kimura S, Tomobe Y, Kobayashi M, Mitsui Y, et al. A novel potent vasoconstrictor peptide produced by vascular endothelial cells. Nature 1988;332(6163):411–15.

[40] Ito H, Hirata Y, Hiroe M, Tsujino M, Adachi S, Takamoto T, et al. Endothelin-1 induces hypertrophy with enhanced expression of muscle-specific genes in cultured neonatal rat cardiomyocytes. Circ. Res. 1991;69(1):209–15.

[41] Jones LG, Rozich JD, Tsutsui H, Cooper G. Endothelin stimulates multiple responses in isolated adult ventricular cardiac myocytes. Am. J. Physiol. 1992;263(5):H1447–54 Pt 2.

[42] Lagerqvist EL, Finnin BA, Pouton CW, Haynes JM. Endothelin-1 and angiotensin ii modulate rate and contraction amplitude in a subpopulation of mouse embryonic stem cell-derived cardiomyocyte-containing bodies. Stem Cell Res. 2011;6(1):23–33.

[43] Kapoor N, Maxwell JT, Mignery GA, Will D, Blatter LA, Banach K. Spatially defined insp3-mediated signaling in embryonic stem cell-derived cardiomyocytes. PLoS One 2014;9(1):e83715.

[44] Sequeira V, Witjas-Paalberends ER, Kuster DW, van der Velden J. Cardiac myosin-binding protein C: hypertrophic cardiomyopathy mutations and structure-function relationships. Pflug. Arch. 2014;466(2):201–6.

[45] Helms AS, Tang VT, O'Leary TS, Friedline S, Wauchope M, Arora A, et al. Effects of MYBPC3 loss-of-function mutations preceding hypertrophic cardiomyopathy. JCI Insight 2020;5(2).

[46] Birket MJ, Ribeiro MC, Kosmidis G, Ward D, Leitoguinho AR, van de Pol V, et al. Contractile defect caused by mutation in MYBPC3 revealed under conditions optimized for human PSC-Cardiomyocyte function. Cell Rep. 2015;13(4):733–45.

[47] Smal I, Carranza-Herrezuelo N, Klein S, Wielopolski P, Moelker A, Springeling T, et al. Reversible jump mcmc methods for fully automatic motion analysis in tagged mri. Med. Image Anal. 2012;16(1):301–24.

[48] Toepfer CN, Sharma A, Cicconet M, Garfinkel AC, Mucke M, Neyazi M, et al. SarcTrack. Circ. Res. 2019;124(8):1172–83.

[49] Kumar N, Dougherty JA, Manring HR, Elmadbouh I, Mergaye M, Czirok A, et al. Assessment of temporal functional changes and miRNA profiling of human iPSC-derived cardiomyocytes. Sci. Rep. 2019;9(1):13188.

[50] Scalzo S, Afonso MQL, da Fonseca NJ, Jesus ICG, Alves AP, Mendonça C, et al. Dense optical flow software to quantify cellular contractility. Cell Rep. Methods 2021;1(4):100044.